Immunopathologia Persa
DOI:10.34172/ipp.2024.40596
http immunopathol.com

The enhancement of therapeutic effects of low-intensity ultrasound with spiky and spherical gold nanoparticles on CT26 cell line; an in vitro study

Molood Gooniband Shooshtari[1], Mohammad Bagher Shiran[2*], Sakine Shirvalilou[2]

[1]Department of Medical Physics, School of Medicine, Iran University of Medical Sciences, Tehran, Iran
[2]Finetech in Medicine Research Center, Iran University of Medical Sciences, Tehran, Iran

***Correspondence to**
Mohammad Bagher Shiran,
Email: baghershiran@gmail.com, Shiran.m@iums.ac.ir

Received 9 Sep. 2023
Accepted 21 Nov. 2023
ePublished 29 Jan. 2024

Keywords: Spiky gold nanoparticles, Spherical gold nanoparticles, Low-intensity ultrasound, None-thermal effects of ultrasound, CT26 cells

Abstract

Introduction: The utilization of combination therapy has gained attention in the medical field as it can enhance treatment efficacy while minimizing side effects. Gold nanoparticles (AuNPs) have been identified as a promising candidate for enhancing the bioeffects of ultrasound (US) waves.
Objectives: The primary objective of this study was to examine the impact of US irradiation when combined with spiky and spherical AuNPs on CT26 cells.
Materials and Methods: Following a tailored composition, we devised and produced AuNPs with spiky and spherical morphologies. The properties of these nanoparticles were assessed using dynamic light scattering (DLS), voltammetry, and transmission electron microscopy (TEM). The CT26 cells were treated with the two types of nanoparticles and subsequently exposed to US radiation (1 W/cm^2, 1 MHz, and 10 minutes). The cytotoxic effects of various therapeutic interventions were assessed using MTT and flow cytometry assays.
Results: This study's findings indicate that nanoparticles' morphology played a significant role in influencing the antitumor effects of US. Specifically, it was observed that the presence of spiky nanoparticles, when subjected to US, resulted in a significantly higher rate of cell death compared to spherical nanoparticles ($P<0.001$). Additionally, it was observed that the temperature changes induced by the spiky nanoparticles were comparatively lower. This observation implies that nanoparticles with spiky morphology enhance the non-thermal effects of US waves.
Conclusion: The outcomes demonstrate a noteworthy augmentation in the biological impacts, specifically the non-thermal effects of US waves when employed in conjunction with spiky nanoparticles.

Citation: Gooniband Shooshtari M, Shiran MB, Shirvalilou S. The enhancement of therapeutic effects of low-intensity ultrasound with spiky and spherical gold nanoparticles on CT26 cell line; an in vitro study. Immunopathol Persa. 2024;10(2):e40596. DOI:10.34172/ipp.2024.40596.

Introduction

Despite the considerable endeavors and swift progressions in medical technology, cancer remains the second most prevalent cause of mortality worldwide (1). The effectiveness of conventional treatment modalities is constrained due to various factors. However, advancements in biomedicine have led to the emergence of novel therapeutic approaches to facilitate the desired outcomes (2). In contemporary medical practice, ultrasound (US) radiation has gained significant prominence due to its notable attributes, including its non-invasive and non-ionizing nature. This has led to its extensive application in both therapeutic and diagnostic contexts, encompassing a range of frequencies and intensities (3). The impacts of US irradiation can be broadly categorized into thermal and non-thermal effects, resulting in alterations to the functionality and structure of biosystems (4,5). The thermal effects of US pertain to an increase in temperature, while the non-thermal effects of US are ascribed to acoustic streaming and acoustic radiation force. These non-thermal effects encompass diverse mechanisms that give rise to the generation of shock waves and microjets, leading to mechanical harm to the surrounding tissue (6). In general, it is widely believed that the mechanical impacts of US can be attributed to acoustic cavitation, a phenomenon that is recognized as a threshold occurrence (7). Gas

Key point

Integrating nanoparticles with US irradiation has been the subject of ongoing research and development. It was observed that the presence of spiky nanoparticles enhances the non-thermal effects of US waves and results in a significant rate of cell death.

bubbles that are generated within an ultrasonic field have the ability to undergo growth, oscillation, and subsequent collapse. The collapse of the medium leads to a significant increase in temperature and pressure, resulting in the generation of highly intense shear stresses and shock waves. Following this, the collapse of bubbles has a detrimental impact on neighboring cells, potentially leading to fatality in certain cases (8). In recent years, the application of nanotechnology has significantly transformed the conceptual framework of conventional therapy. This transformation has been achieved through the development of safer and more efficient nanomedicines, which involve the cultivation of innovative nanosized materials. A novel approach involving the utilization of nanoparticles to enhance the efficacy of US waves has emerged. Based on multiple investigations, it has been observed that nanoparticles have the ability to effectively modulate the process of cavitation by reducing the threshold necessary for the initiation of cavitation nucleation (9,10). Numerous scholars have conducted extensive investigations on diverse nanomaterials. Among these, gold nanoparticles (AuNPs) have garnered considerable interest and have emerged as a prominent focus in cancer research. This is primarily attributed to their appealing characteristics, including elevated biocompatibility, efficient uptake, minimal toxicity, and straightforward synthesis (11,12). Furthermore, it is widely believed that AuNPs have the ability to simultaneously amplify the thermal and mechanical impacts of US waves. Previous researches have demonstrated that the application of low-intensity US can result in cell death, even in the absence of significant temperature elevation, both with and without the presence of nanoparticles (3,13).

Objectives

The presence of nanoparticles can augment the rate of cell death induced by US through the thermal and mechanical interaction of US waves. It is highly probable that the implementation of spiky nanoparticles can yield even greater effects. This phenomenon occurs due to the elevated surface roughness of spiky nanoparticles, which effectively enhances the formation of voids, facilitating the initiation of cavitation. Consequently, the mechanical integrity of the cell membrane is compromised, leading to eventual cell lysis.

Materials and Methods

Synthesis of gold nanoparticles

The materials and procedures utilized in the synthesis of AuNPs were obtained from Sigma-Aldrich. The materials included ascorbic acid, silver nitrate, chloroauric acid trihydrate, trisodium citrate dehydrate (sodium citrate), hydrogen peroxide (30%), sulfuric acid (98%), hydrochloric acid (37%), and nitric acid (70%). To prepare the stock solution of AuNPs, a mixture of 50 mg of HACl4.3H2O and 25 mL of distilled water was employed, resulting in the formation of a gold (III) ion stock solution with a concentration of 5.0 mM. A 1.5 M trisodium citrate solution was prepared by dissolving 22 g of sodium citrate in 50 mL of distilled water. It is recommended to prepare fresh solutions of sodium citrate prior to each synthesis due to inadequate maintenance of the solution in the laboratory. Following the cleaning of the glassware using Piranha solution and subsequent rinsing with water, a volume of 5 mL of HAuCl4 was introduced into a 10 mL Erlenmeyer flask under continuous stirring on a heated plate. Subsequently, the solution was subjected to heat until it reached its boiling point, while concurrently incorporating a magnetic stirring bar. Subsequently, a volume of 50 µL of trisodium citrate dehydrate solution (1.5 M) was introduced into the vigorously agitated gold solution that was undergoing boiling. The AuNPs were synthesized through the reduction of gold (III) by citrate. Following the change in color of the solution to red, the process of heating was terminated. The synthesis of a stock solution of spiky AuNPs was conducted by dissolving 11.8 mg of HAuCl4.3H2O in 1.5 mL of distilled water, resulting in a hydrogen tetrachloroaute-based stock solution with a concentration of 19.97 mM of gold (III) ions. Through the amalgamation of 1 mg of silver nitrate ($AgNO_3$) with 2 mL of distilled water, a solution of silver nitrate with a concentration of 2.9 mM was successfully generated. A solution of ascorbic acid with a concentration of 39.75 mM was prepared by dissolving 10.5 mg of ascorbic acid in 1.5 mL of distilled water. To complete the mixture, a solution of polyvinylpyrrolidone (PVP) with a concentration of 1.5% was prepared by dissolving 150 mg of PVP in 1 mL of distilled water. A 250 mL Erlenmeyer flask was initially filled with 150 mL of distilled water, followed by the addition of 5 mL of AuNPs as a seed. Subsequently, the mixture was administered 1.5 mL of a gold ion solution with a concentration of 19.97 mM, along with 150 µL of a hydrochloric acid solution with a concentration of 1 M. Subsequently, an aliquot of 1685 µL from a silver nitrate solution with a concentration of 2.9 mM was introduced. After 60 seconds, the resulting solution was combined with 1500 µL of ascorbic acid with a concentration of 39.75 mM, leading to the manifestation of a blue discoloration. Following a 10-second interval, a 1 mL volume of a 1.5% PVP solution was introduced into the mixture, which was concurrently subjected to stirring for a duration of 2 hours. Finally, the solution underwent centrifugation for a duration of 60 minutes at a force of 6000 g (14).

Gold nanoparticles characterization

The morphological characteristics of the nanoparticles were examined through the utilization of a transmission electron microscope (TEM, Zeiss LEO906, Germany). The effective diameter of nanoparticles was measured using dynamic light scattering (DLS) with the Malvern Zetasizer

Nano ZS-90 instrument. Measurements were conducted to determine the zeta potentials associated with the surface charge of nanoparticles.

Cell culture

The murine cell line CT26, which is commonly employed for colon cancer modeling, was cultivated in RPMI 1640 medium. The medium was supplemented with fetal bovine serum (10%), penicillin (100 u/mL), and streptomycin (100 mg/mL). The cell culture was maintained in a humidified incubator set at 37 °C with 5% CO2. The cells were subjected to trypsinization using a solution containing 1 mM EDTA in 0.25% trypsin (w/v) in phosphate-buffered saline (PBS), followed by collection.

Calibration of ultrasound generator

The calibration and measurement of the power output of the US generator (Phyaction 190i, Germany) were conducted using the radiation force method. The generator was equipped with a circular probe, which had an area of 1 cm^2 and operated at an intensity of 1 W/cm^2 in continuous wave mode at a frequency of 1 MHz. The following equation was then used to calculate the linear relationship between nominal intensity (I_1) and intensity (I_2):

$I_1 = 0.953I_2 + 0.135$, $R^2 = 0.974$

The dye paper method was utilized to compute the ratio of peak intensity to average intensity (Ip/Ia). The approximate value of Koss off was approximately 5.

In vitro experiments

In vitro cytotoxicity assay of nanoparticles

The cytotoxicity of nanoparticles was assessed using an in vitro experiment, specifically the MTT assay. Moreover, CT26 cells were cultured in 96-well plates and incubated for a duration of 24 hours. Subsequently, the culture medium was substituted with an alternative medium containing gold nanoparticle of both spherical and spiky morphology, with concentrations ranging from 0.15 to 10 µg/mL, each in separate flasks. The flasks were then incubated for a duration of 24 hours. Following the removal of the medium, the wells were rinsed with PBS and subsequently incubated at a temperature of 37 °C for a period of 4 hours with 20 µL of MTT (5 mg/mL). The insoluble formazan crystals were dissolved by the addition of 100 µL of dimethyl sulfoxide (DMSO) to the wells. Subsequently, the absorbance of each well was assessed using a microplate reader (BioTek, USA) configured to measure at a wavelength of 570 nm. The IC50 values for AuNPs with spherical and spiky morphologies were determined through calculation.

Ultrasound treatment of the cells

The CT26 cells (10×10^4 cells) were seeded in a petri dish with a diameter of 3 cm and placed at the last axial maximum of the transducer via a custom-made adaptor. The cell petri dish was positioned onto the adaptor, which had been pre-filled with distilled water in preparation for sonication. Care was taken to ensure the presence of air trapped between the petri dish and the adaptor. The temperature variations at various levels of intensity and durations of sonication were observed using a digital thermometer (Hanyoung, Korea, NX4) with a sensitivity of ± 0.1 °C. This thermometer was connected to a thermocouple measuring 125 µm in diameter, which was attached to the lower surface of the petri dish. To mitigate the occurrence of standing waves, the experimental setup involved the introduction of cultured medium and acoustic gel into the petri dish. Additionally, a rubber cover with a thickness of 5 mm was employed to seal the petri dish. The experimental procedure involved subjecting all cellular samples, comprising both gold nanoparticle-infused cells of varying shapes and cells without AuNPs, to a continuous wave-mode US at an intensity of 1 W/cm^2 for a duration of 10 minutes. In order to assess the viability of the cells, the sonicated cells were subjected to a 24-hour incubation period to facilitate attachment to the petri dish. Following a 24-hour incubation period, distinct types of AuNPs, namely spherical and spiky, were individually introduced to the cellular environment at a concentration equivalent to the IC50 value. Following a 24-hour incubation period, the cells were rinsed with PBS and subsequently supplemented with a fresh culture medium. The therapeutic effects were assessed through the utilization of viability assays, specifically the MTT test and Annexin V-FITC/PI fluorescent staining analysis.

In vitro anti-tumor efficacy

Viability assay by MTT test

CT26 cells were cultured in petri dishes with a diameter of 3 cm, at a density of 10×10^4 cells. Following the introduction of nanoparticles and subsequent exposure to US irradiation, cellular specimens were collected and subsequently transferred to a 96-well plate. Following the cellular washing procedure, a concentration of 5 mg/mL of MTT was introduced into the wells, and the cells were subsequently incubated for a duration of 4 hours under dark conditions at a temperature of 37 °C. Subsequently, the MTT solution was removed and replaced with 100 µL of DMSO to facilitate the dissolution of formazan crystals. Following a 15-minute incubation period, the absorbance was quantified using spectrophotometry at a wavelength of 570 nm. In order to construct cell viability curves, we employed a normalization technique by comparing our measurements to those obtained from control cells.

Flowcytometry analysis of cell apoptosis

The rate of apoptotic and necrotic cell death was evaluated in response to various treatments using the conventional

flow cytometry assay, employing Annexin V-FITC/PI. Following cell counting and PBS washing, the cells were suspended in ice-cold 1 × binding buffer. Subsequently, a 15-minute incubation in the dark at room temperature was carried out, during which 5 µL of annexin V-FITC was added. Following an additional cycle of washing and resuspension in a 1 × binding buffer, the cells were subjected to staining using 5 µL of propidium iodide (PI). The resulting fluorescence was then measured using a BD FACSCalibur™ flow cytometer (BD, San Jose, CA, USA). Cells that exhibited positive staining for annexin V-FITC but negative staining for PI were classified as being in the early apoptotic stage. Nevertheless, the presence of dual-positive staining was regarded as an indicative characteristic of apoptosis in its advanced stages. Additionally, the cells undergoing necrosis were identified and labeled as positive for PI.

Statistical analysis

The statistical analysis involved conducting all experiments in triplicate and presenting the resulting data as mean ± SD (standard deviation) using GraphPad Prism software. A P value of <0.05 was considered statistically significant.

Results

Characterization of the nanoparticles

The results provide information regarding the particle size and zeta potential of two types of AuNPs: spiky and spherical. The average particle size for spherical nanoparticles was determined to be 75.78 ± 5.6 nm, while for spiky nanoparticles it was found to be 84.98 ± 6.4 nm. Furthermore, it was observed that both spiky (-9.58 mV) and spherical (-6.20 mV) nanoparticles exhibited negative zeta potentials. Figure 1 displays transmission electron microscopy (TEM) images of nanoparticles. The TEM images provided conclusive evidence that both nanoparticles exhibited excellent dispersion and exhibited consistent shapes. The uniformity of spiky shapes was of utmost importance in this study, and its achievement posed several challenges during the synthesis process. In a comparative manner, the aforementioned sizes exhibited a greater magnitude in relation to the size ascertained through TEM images. The observed variations may have arisen due to the uptake of liquid by the nanoparticles during the DLS analysis (Figure 1).

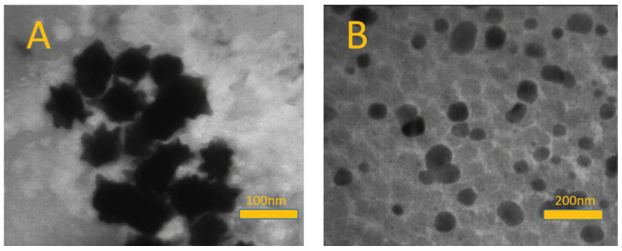

Figure 1. TEM images of nanoparticles. (A) Spiky AuNPs, (B) spherical AuNPs.

In vitro cytotoxicity assay of nanoparticles

The cytotoxicity of spiky and spherical AuNPs on CT26 cells was assessed using the MTT assay in an in vitro setting. In pursuit of this objective, diverse concentrations of both spiky and spherical AuNPs were employed for the purpose of treating the subject matter. Figure 2 illustrates the impact of nanoparticle concentrations on the rate of cell viability following 24-hour treatments. As illustrated in Figure 2, the cytotoxicity of both spherical and spiky nanoparticles was found to be dependent on their concentration. The IC50 values of AuNPs with spiky and spherical morphologies were determined by analyzing the cytotoxicity data, and were subsequently utilized in the development of therapeutic strategies. The study revealed that the cytotoxicity of spherical nanoparticles, across all concentrations employed, surpasses that of spiky nanoparticles. The findings presented in Figure 2 indicate that the IC50 value for spherical nanoparticles is 1 ± 0.12 µg/mL, whereas the IC50 value for spiky nanoparticles is 3.2 ± 0.10 µg/mL. This suggests that a threefold greater quantity of spiky nanoparticles is necessary ($P<0.05$) compared to spherical nanoparticles in order to achieve equivalent cytotoxicity on CT26 cells.

Time-temperature profile

The time-temperature profile depicts the variations in temperature experienced by cells subjected to different treatments, as illustrated in Figure 3. Based on the temperature profile analysis of CT26 cells, it was observed that the average temperature increase in the absence of nanoparticles was 3.23 ± 0.15 °C. The average temperature increases observed for spherical and spikey AuNPs introduced into cells 24 hours before subjecting them to sonication were 3.63 ± 0.25 °C and 2.16 ± 0.15 °C, respectively. One notable observation was that the increase in temperature of the cells containing spiky AuNPs was comparatively lower when compared to cells containing spherical AuNPs or cells without any nanoparticles. The temperature increase for each treatment is recorded and presented in Table 1.

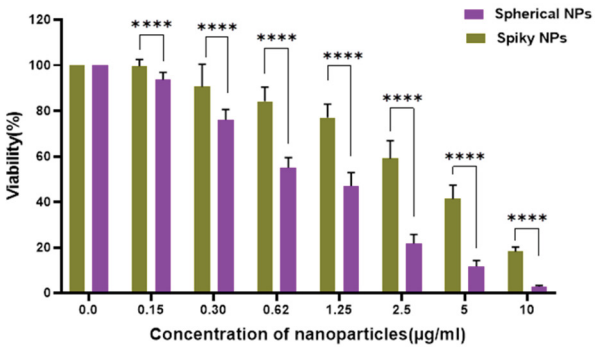

Figure 2. MTT assays of the CT26 cells treated with different concentrations of spiky and spherical AuNPs. Statistical significance was showed with **** $P < 0.0001$ respectively.

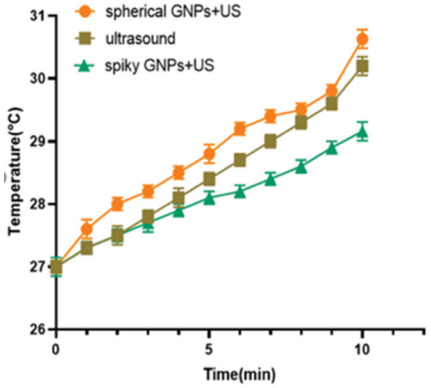

Figure 3. Time-Temperature profile of different treatments by 10 min sonication.

In vitro anti-tumor efficacy

Viability assay by MTT test

The present study aimed to evaluate the anti-tumor efficacy and viability of spiky and spherical AuNPs through an in vitro assay using the MTT test. Specifically, the cytotoxic effects of these nanoparticles were examined in the presence of US irradiation. As previously stated, the IC50 values of both spiky and spherical nanoparticles were utilized in the treatments. The findings depicted in Figure 4 illustrate the impact of nanoparticles on the reduction of cell viability when combined with US compared to the use of US alone, with statistical significance ($P<0.05$). According to the findings, the introduction of spiky nanoparticles led to a notable decrease in cell viability. Specifically, the viability of cells exposed to spiky nanoparticles combined with ultrasonic treatment decreased to 55.73 ± 6.03%. In comparison, the viability of cells treated with spherical nanoparticles and US was slightly higher at 71.2 ± 5.85%. Notably, the cell viability for US sonication without the presence of any nanoparticles was measured at 83.2 ± 8.6%. Based on the findings of this study, it was observed that the utilization of spiky nanoparticles led to a notable decrease in cell count upon exposure to US ($P<0.001$).

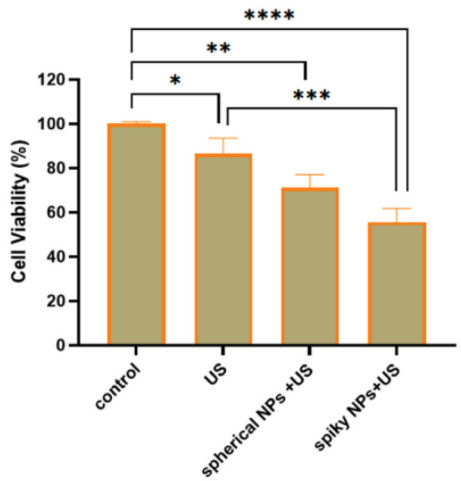

Figure 4. MTT assays of the CT26 cells by different treatments. Data were presented as mean ± SD of three experiments. Statistical significance was showed with * P <0.05, ** P < 0.01, *** P < 0.001, and **** P < 0.0001, respectively.

Table 1. Temperature raises in different treatments by 10 min sonication

Treatments	Temperature rising
Spherical nanoparticles + ultrasound	3.63±0.25
Spiky nanoparticles + ultrasound	2.16±0.15
Ultrasound irradiation (without nanoparticles)	3.23±0.15

Flowcytometry analysis of cell apoptosis

The apoptosis and necrosis of CT26 cells following various treatments were evaluated using an Annexin V-FITC/PI-based flow cytometry assay. The process of evaluating cell death, including early apoptosis, late apoptosis, and necrosis, is depicted in Figures 5 and 6. The experimental results demonstrate that the treatment involving spiky nanoparticles combined with US resulted in the highest percentage of cell death, with a value of 44.2 ± 0.47%. In comparison, the treatment involving spherical nanoparticles combined with US yielded a lower cell death rate of 30.8 ± 0.37%. Conversely, sonicated cells without the addition of any particles, regardless of their shape, exhibited a significantly lower cell death rate of 12.77 ± 0.9%. The findings of this study provide confirmation of the involvement of AuNPs in augmenting the effects of US. However, the utilization of Spiky nanoparticles and US irradiation significantly intensified the cytotoxicity of the cells.

Discussion

The purpose of this study was to assess the cytotoxicity of spiky AuNPs when combined with low-intensity US irradiation, as it is believed that combination therapy can enhance treatment efficacy while minimizing side effects. The investigation was conducted in an in-vitro setting. The present study involved subjecting cells containing AuNPs of varying shapes to continuous wave-mode US at an intensity of 1 W/cm^2 for a duration of 10 minutes. Table 1 demonstrates the comparative thermal enhancement function of spherical AuNPs in relation to exposure to US alone. As depicted in Table 1, the observed temperature elevation of spiky AuNPs exhibited a lesser magnitude compared to both spherical AuNPs and pure water. There exist multiple potential factors contributing to the reduced temperature increase observed in spiky nanoparticles. The influence of thermal conductivity can be attributed to the shape of nanoparticles. Hamilton and Crosser designed a steady-state apparatus to investigate suspensions containing millimeter-sized spherical and non-spherical particles. Their study revealed that the thermal conductivity of the suspension may be influenced by the shape of the dispersed particles (15). Additionally, the observed negative trend in thermal conductivity may be attributed to the inherent characteristics and

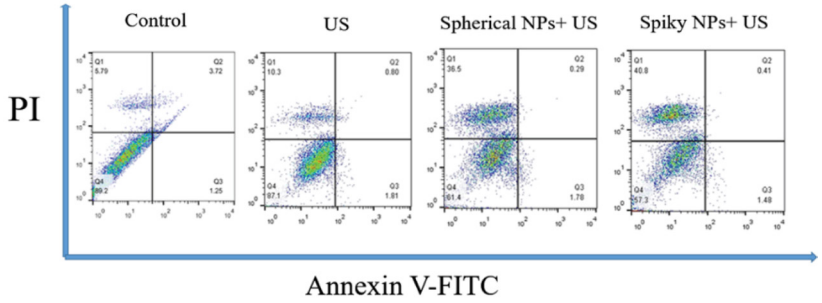

Figure 5. Annexin V-FITC/PI staining assay for detection of apoptosis and necrosis of CT26 cells by different treatments. PI, propidium iodide.

arrangement of nanoparticles. Specifically, the existence of distinct energy levels in the electronic structure can lead to this phenomenon. The arrangement of these energy levels in proximity to the highest occupied level is highly susceptible to variations in shape and size, which in turn can be influenced by thermal, chemical, and electrochemical properties (16). The cytotoxicity levels of spherical and spiky nanoparticles were assessed using the MTT test at the same concentration. Figure 2 illustrates that these nanoparticles exhibited varying degrees of cytotoxicity. Notably, spherical nanoparticles consistently displayed higher levels of cytotoxicity compared to spiky nanoparticles across all tested concentrations. The IC50 values of spherical nanoparticles were determined to be 1 ± 0.12 µg/mL, whereas the IC50 values of spiky nanoparticles were found to be 3.2 ± 0.10 µg/mL ($P < 0.01$). The observed variations can be attributed to a range of factors, as documented in prior research (17,18). The dimensions, morphology, and surface characteristics of nanoparticles play a crucial role in influencing their toxicological properties, cellular internalization rate, distribution within the body, and biological reactivity. Regarding the size-dependent cytotoxicity, previous research (19,20) conducted experiments using four distinct

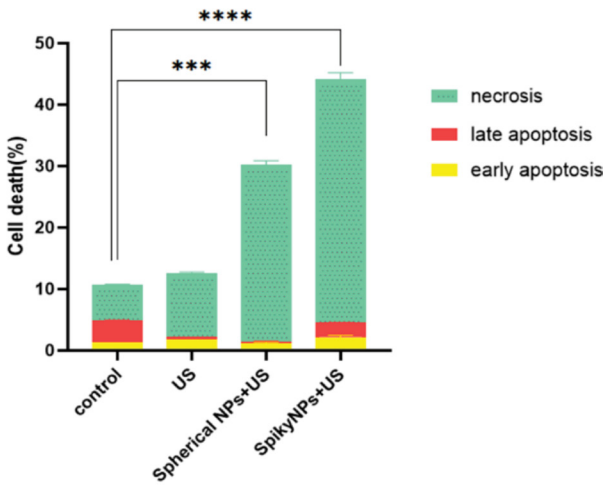

Figure 5. Annexin V-FITC/PI staining assay for detection of apoptosis and necrosis of CT26 cells by different treatments.

cell lines, namely epithelial cells (HeLa), melanoma cells (SK-Mel-28), macrophages (J774A1), and tissue fibroblasts (L929), to investigate the impact of triphenylphosphine-stabilized AuNPs on cellular response. The findings of these studies suggest that the observed cytotoxicity is influenced by the size of the AuNPs. Also, Dobrovolskaia et al (12) reported that the toxicity of AuNP varies as a result of particle shapes. The study conducted by Kosheleva et al (21) investigated the impact of combining AuNPs with low-intensity US on lung cancer cells. The objective was to ascertain whether the introduction of nanoparticles specifically augmented the cytotoxicity against cancer cells. The findings of their study demonstrated that the utilization of nanoparticles (at a concentration of 2.5 µg/mL and a size of 10 nm) in conjunction with US radiation (at a frequency of 4 MHz and power of 8 W) resulted in a significant decrease in the occurrence of A549 lung cancer cells, reducing the prevalence from 60.5% to 29.8%. The findings of the study indicate that spiky nanoparticles exhibit enhanced effectiveness in inducing cell death. It was observed that the presence of spiky nanoparticles led to an increased occurrence of cavitation, a phenomenon characterized by the formation, growth, oscillation, and subsequent collapse of bubbles. The process of collapsing resulted in the generation of significant shear stresses and shock waves, which in turn had the potential to cause substantial damage to adjacent cells (22). The experimental results demonstrate that the presence of spiky AuNPs at a lower temperature leads to a decrease in cell viability. This reduction is more pronounced compared to the increased temperature observed with spherical nanoparticles and even in the absence of nanoparticles. The higher efficacy of treatment is evidenced by both the MTT assay and the flow cytometry test. These findings highlight the significant contribution of spiky nanoparticles in augmenting the non-thermal effects of US. The non-thermal mechanisms that have been identified are multifaceted and encompass various sets of mechanisms, such as radiation forces, stable and inertial cavitation, and microstreaming (23). This implies that the presence of spiky nanoparticles in conjunction with US has resulted in the augmentation of one or more of these mechanisms.

Conclusion

In conclusion, the utilization of nanoparticles in conjunction with US irradiation represents a promising field of investigation. Building upon previous research that has demonstrated the potential of nanoparticles in augmenting the effects of US, the present study aimed to investigate the impact of spiky AuNPs on the therapeutic efficacy of US. The findings demonstrated a notable improvement in the therapeutic effectiveness of US in enhancing the non-thermal effects of ultrasound.

Limitations of the study

The uniformity of spiky shapes was of utmost importance in this study, and its achievement posed several challenges during the synthesis process**.**

Authors' contribution

Conceptualization: Mohammad Bagher Shiran, Sakine Shirvalilou.
Data curation: Molood Gooniband Shooshtari, Sakine Shirvalilou.
Formal analysis: Molood Gooniband Shooshtari.
Funding acquisition: Mohammad Bagher Shiran.
Investigation: Mohammad Bagher Shiran, Sakine Shirvalilou, Molood Gooniband Shooshtari.
Methodology: Mohammad Bagher Shiran, Sakine Shirvalilou .
Project administration: Mohammad Bagher Shiran, Sakine Shirvalilou.
Resources: Mohammad Bagher Shiran.
Software: Molood Gooniband Shooshtari.
Supervision: Mohammad Bagher Shiran.
Validation: Mohammad Bagher Shiran, Sakine Shirvalilou.
Visualization: Mohammad Bagher Shiran, Molood Gooniband Shooshtari.
Writing–original draft: Molood Gooniband Shooshtari.
Writing–review & editing: Mohammad Bagher Shiran, Sakine Shirvalilou.

Conflicts of interest

The authors have no conflicts of interest.

Ethical issues

The research conducted in this study adhered to the principles outlined in the Declaration of Helsinki and was approved by the Ethics Committee of Iran University of Medical Sciences (Ethical code#IR.IUMS.FMD. REC.1400.072). Accordingly, written informed consent was taken from all participants before any intervention. This study was extracted from PhD thesis of Molood Gooniband Shooshtari (Thesis# 19350) at the department of medical physic of Iran University of Medical Sciences. The authors have fully complied with ethical issues, such as plagiarism, data fabrication, and double publication.

Funding/Support

This work was supported by a (Grant#19350) from Iran University of Medical Sciences (IUMS).

References

1. Lin L, Li Z, Yan L, Liu Y, Yang H, Li H. Global, regional, and national cancer incidence and death for 29 cancer groups in 2019 and trends analysis of the global cancer burden, 1990-2019. J Hematol Oncol. 2021;14:197. doi: 10.1186/s13045-021-01213-z.
2. Lyatskaya Y, Winey B, Kiger WS 3rd, Hurwitz M, Zygmanski P, Makrigiorgos GM, et al. Combined clinical and research training in medical physics in a multi-institutional setting: 13-year experience of Harvard Medical Physics Residency Program. J Appl Clin Med Phys. 2023;24:e13806. doi: 10.1002/acm2.13806.
3. Feril LB Jr, Kondo T. Biological effects of low intensity ultrasound: the mechanism involved, and its implications on therapy and on biosafety of ultrasound. J Radiat Res. 2004;45:479-89. doi: 10.1269/jrr.45.479.
4. Sarvazyan AP, Rudenko OV, Nyborg WL. Biomedical applications of radiation force of ultrasound: historical roots and physical basis. Ultrasound Med Biol. 2010;36:1379-94. doi: 10.1016/j.ultrasmedbio.2010.05.015.
5. ter Haar G. Ultrasound bioeffects and safety. Proc Inst Mech Eng H. 2010;224:363-73. doi: 10.1243/09544119JEIM613.
6. Holland CK, Apfel RE. Thresholds for transient cavitation produced by pulsed ultrasound in a controlled nuclei environment. J Acoust Soc Am. 1990;88:2059-69. doi: 10.1121/1.400102.
7. Miller MW, Miller DL, Brayman AA. A review of in vitro bioeffects of inertial ultrasonic cavitation from a mechanistic perspective. Ultrasound Med Biol. 1996;22:1131-54. doi: 10.1016/s0301-5629(96)00089-0.
8. Karthikesh MS, Yang X. The effect of ultrasound cavitation on endothelial cells. Exp Biol Med (Maywood). 2021;246:758-770. doi: 10.1177/1535370220982301.
9. Ahmed SE, Martins AM, Husseini GA. The use of ultrasound to release chemotherapeutic drugs from micelles and liposomes. J Drug Target. 2015;23:16-42. doi: 10.3109/1061186X.2014.954119.
10. Chang WH, Sun JS, Chang SP, Lin JC. Study of thermal effects of ultrasound stimulation on fracture healing. Bioelectromagnetics. 2002;23:256-63. doi: 10.1002/bem.10009.
11. Kennedy LC, Bickford LR, Lewinski NA, Coughlin AJ, Hu Y, Day ES, et al. A new era for cancer treatment: gold-nanoparticle-mediated thermal therapies. Small. 2011;7:169-83. doi: 10.1002/smll.201000134.
12. Dobrovolskaia MA, Patri AK, Zheng J, Clogston JD, Ayub N, Aggarwal P, et al. Interaction of colloidal gold nanoparticles with human blood: effects on particle size and analysis of plasma protein binding profiles. Nanomedicine. 2009;5:106-17. doi: 10.1016/j.nano.2008.08.001.
13. Liang S, Deng X, Ma P, Cheng Z, Lin J. Recent Advances in Nanomaterial-Assisted Combinational Sonodynamic Cancer Therapy. Adv Mater. 2020;32:e2003214. doi: 10.1002/adma.202003214.
14. Nam J, Son S, Moon JJ. Adjuvant-Loaded Spiky Gold Nanoparticles for Activation of Innate Immune Cells. Cell Mol Bioeng. 2017;10:341-355. doi: 10.1007/s12195-017-0505-8.
15. attnaik PK, Abbas MA, Mishra S, Khan SU, Bhatti MM. Free Convective Flow of Hamilton-Crosser Model Gold-water Nanofluid Through a Channel with Permeable Moving Walls. Comb Chem High Throughput Screen. 2022;25:1103-1114. doi: 10.2174/1386207324666210813112323.
16. Shalkevich N, Escher W, Bürgi T, Michel B, Si-Ahmed L, Poulikakos D. On the thermal conductivity of gold nanoparticle colloids. Langmuir. 2010 Jan 19;26:663-70. doi: 10.1021/la9022757.
17. Potenza MAC, Krpetić Ž, Sanvito T, Cai Q, Monopoli M, de Araújo JM, et al. Detecting the shape of anisotropic gold nanoparticles in dispersion with single particle extinction and scattering. Nanoscale. 2017 Feb 23;9:2778-2784. doi: 10.1039/c6nr08977a.
18. Muraca F, Boselli L, Castagnola V, Dawson KA. Ultrasmall Gold Nanoparticle Cellular Uptake: Influence of Transient Bionano Interactions. ACS Appl Bio Mater. 2020;3:3800-3808.

doi: 10.1021/acsabm.0c00379.
19. Pan Y, Neuss S, Leifert A, Fischler M, Wen F, Simon U, et al. Size-dependent cytotoxicity of gold nanoparticles. Small. 2007;3:1941-9. doi: 10.1002/smll.200700378.
20. Chen YS, Hung YC, Liau I, Huang GS. Assessment of the In Vivo Toxicity of Gold Nanoparticles. Nanoscale Res Lett. 2009;4:858-864. doi: 10.1007/s11671-009-9334-6.
21. Kosheleva OK, Lai TC, Chen NG, Hsiao M, Chen CH. Selective killing of cancer cells by nanoparticle-assisted ultrasound. J Nanobiotechnology. 2016;14:46. doi: 10.1186/s12951-016-0194-9.
22. Paliwal S, Mitragotri S. Ultrasound-induced cavitation: applications in drug and gene delivery. Expert Opin Drug Deliv. 2006;3:713-26. doi: 10.1517/17425247.3.6.713.
23. Canavese G, Ancona A, Racca L, Canta M, Dumontel B, Barbaresco F, et al. Nanoparticle-assisted ultrasound: A special focus on sonodynamic therapy against cancer. Chem Eng J. 2018;340:155-172. doi: 10.1016/j.cej.2018.01.060.